# Hard and elastic amorphous carbon nitride thin films studied by $^{13}C$ nuclear magnetic resonance spectroscopy

W. J. Gammon,[1] D. I. Malyarenko,[2] O. Kraft,[3] G. L. Hoatson,[1] A. C. Reilly,[1] and B. C. Holloway[2]
[1]*Department of Physics, College of William & Mary, P.O. Box 8795, Williamsburg, Virginia 23187*
[2]*Department of Applied Science, College of William & Mary, P.O. Box 8795, Williamsburg, Virginia 23187*
[3]*Max-Planck-Institut fur Metallforschung, Stuttgart, Germany*
(Received 18 April 2002; published 3 October 2002)

The chemical bonding of hard and elastic amorphous carbon nitride ($a$-$CN_x$) thin films was examined using solid-state $^{13}C$ NMR spectroscopy. The films were deposited by DC magnetron sputtering in a pure nitrogen discharge on Si(001) substrates at 300 °C. Nanoindentation tests reveal a recovery of 80%, a hardness of 5 GPa, and an elastic modulus of 47 GPa. This combination of low modulus and high strength means the material can be regarded as hard and elastic; the material gives when pressed on and recovers its shape when the load is released. The $^{13}C$ NMR results conclusively demonstrate that hard and elastic $a$-$CN_x$ has an $sp^2$ carbon bonded structure and that $sp^3$ hybridized carbons are absent. Our results stand in contrast with earlier work that proposed that the interesting mechanical properties of hard and elastic $a$-$CN_x$ were due, in part, to $sp^3$ bonded carbon.

DOI: 10.1103/PhysRevB.66.153402 PACS number(s): 81.05.Tp, 81.15.Cd, 62.20.−x, 76.60.Cq

## I. INTRODUCTION

Amorphous carbon nitride ($a$-$CN_x$) thin films are currently being extensively studied because of their unusual mechanical properties. When deposited under suitable deposition conditions, hard and elastic $a$-$CN_x$ films can be fabricated which exhibit high elastic recovery.[1–4] The most widely accepted model that correlates the structure of hard and elastic $a$-$CN_x$ with its mechanical properties proposes that the material consists of buckled graphitic segments with incorporated nitrogen, and that these segments are cross-linked by $sp^3$ bonded carbon.[1,2,5,6] Electron energy loss spectroscopy[2,7,8] (EELS) and near-edge x-ray absorption fine-structure spectroscopy[3,9] (NEXAFS) have been used to try to examine the relative fractions of $sp^2$ and $sp^3$ hybridized carbon bonded to carbon in $a$-$CN_x$. However to date, no reliable quantitative measurements of the amount of $sp^3$ hybridized carbon has been reported in the literature. Recent experiment evidence indicates that an $sp^3$ coordinated carbon environment will relax to $sp^2$ in the presence of approximately 14% nitrogen,[10] and these calculations suggest that $sp^3$ carbon is not stable in hard and elastic $a$-$CN_x$, which exhibits a typical atomic nitrogen concentration of ~20%.[2–4] The focus of this report is to resolve this controversy by the use of solid-state nuclear magnetic resonance spectroscopy (NMR).

Since the NMR chemical shift of $sp^2$ and $sp^3$ bonded carbons are well resolved, other researchers have employed solid-state $^{13}C$ NMR techniques to investigate $a$-$CN_x$ films.[11–14] However, all earlier NMR work on carbon nitride has focused on hydrogenated materials or materials deposited at ambient temperature.[11–14] Separate results have shown that either of these deposition conditions produces an $a$-$CN_x$ material with less robust mechanical properties.[15,16] In addition, no mechanical testing results were reported for any of the $a$-$CN_x$ materials previously characterized by NMR.[11–14] In this paper, we report $^{13}C$ NMR results on an $a$-$CN_x$ material that is hard and elastic and exhibits a high recovery, as determined by nanoindentation.

## II. EXPERIMENT

The $a$-$CN_x$ thin films were deposited by DC magnetron sputtering in a pure nitrogen discharge at 9 mTorr on 75 mm-diam Si(001) substrates. The substrate, positioned 8 cm from the source, was electrically grounded and heated to 300 °C. The target was a 50 mm-diam and 6.4 mm-thick 99.999% pure graphite disk. Mechanical testing of the $a$-$CN_x$ films was carried out with a MTS NanoXP nanoindentation system using a Berkovich tip. The indentations were performed under a constant strain rate condition by keeping $\dot{P}/P = 0.01\ s^{-1}$, where $\dot{P}$ is the load rate and $P$ the load.

For the NMR experiments, 140 mg of material was obtained by depositing three ~9 $\mu$m-thick films that were subsequently scraped off the substrate. All solid-state NMR measurements were carried out at room temperature using a custom-built spectrometer operating at 7 T ($^1H$ Larmor frequency of 300.07 MHz) and with a $^{13}C$ frequency of 75.46 MHz and $^{14}N$ frequency of 21.68 MHz. The applied radio frequency fields (90° pulse widths) were 71.4 kHz (3.5 $\mu$s) for $^1H$, 62.5 kHz (4 $\mu$s) for $^{13}C$, and 41.7 kHz (6 $\mu$s) for $^{14}N$, respectively. Magic angle spinning (MAS) $^{13}C$ NMR spectra were directly obtained using a Hahn echo pulse sequence and a four-pulse total suppression of a spinning sideband (TOSS) sequence.[17] The $^{13}C$ Hahn echo spectra were compared to both the direct detection and cross polarization (CP) spectra. In addition, a rotational echo adiabatic passage double resonance[18] (REAPDOR) experiment was carried out with a 50 $\mu$s $^{14}N$ contact pulse and dephasing over six rotor cycles, with 180° $^{13}C$ pulses every half rotor period. By exploiting the dipole coupling between $^{13}C$ and $^{14}N$ nuclei, the

 

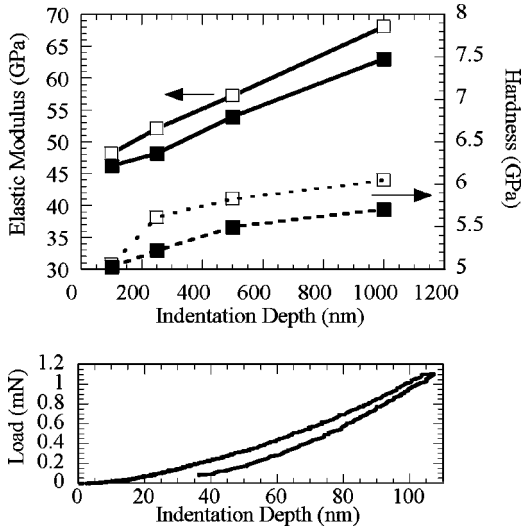


FIG. 1. Nanoindentation results of a 6 $\mu$m-thick $a$-$CN_x$ film. In the upper panel, the hardness (symbols with dashed lines) and elastic modulus (symbols with solid lines) are shown as a function of indentation depth. The open squares correspond to results obtained at the center of the 75 mm-diam substrate, while the filled squares were obtained 10 mm from the edge. The lower panel illustrates a typical load versus displacement curve of the material deposited and characterized in this study.

REAPDOR experiment allows the determination of the portion of the $^{13}C$ spectra originating from carbons bonded to nitrogen. Details of recycle delays ($\tau_d$), echo spacing times ($\tau_e$), spinning speeds ($\nu_r$), and number of scans (NS) for each experiment are included in the figure captions. All spectra were apodized using 200-Hz Lorentzian line broadening, and the $^{13}C$ chemical shift is referenced to tetramethylsilane (TMS at zero ppm).

### III. RESULTS AND DISCUSSION

The elastic modulus and hardness of a 6 $\mu$m-thick $a$-$CN_x$ film, as obtained from the method of Oliver and Pharr,[19] are shown as a function of indentation depth in the upper panel of Fig. 1. The open squares correspond to testing obtained at the center of the 75 mm-diam substrate, while the filled squares correspond to testing 10 mm from the edge. For an indentation depth of 100 nm, nanoindentation tests reveal a hardness of 5 GPa and an elastic modulus of 47 GPa. As the indentation depth increases both the hardness and elastic modulus increase due to the substrate-film interaction. Interestingly, the mechanical properties at the center and edge follow very similar trends except for a constant offset, which we attribute to decreased ion flux near the edge.[20] A typical load versus displacement curve, illustrating the high elastic recovery of this material, is shown in the lower panel of Fig. 1. The unloading portion of the curve was fitted with the power-law relation as described by Oliver and Pharr.[19] A power-law exponent of 2.2 was found to best describe the contact area of the indenter tip for this material. Using this exponent, the residual displacement was determined by the best least-squares fit. Averaging over 10 indents, the recovery, as defined by Zheng *et al.*,[21] was found to be (80.0 $\pm$0.6)% and (82$\pm$2)% near the center and edge of the 75 mm-diam substrate, respectively, with an indentation depth of 100 nm with a maximum load of $\sim$1.0 mN. Comparison of the mechanical properties from center to edge of the substrate demonstrates that our material collection process for the NMR experiments was reasonable. We have produced large-area, highly elastic $a$-$CN_x$ films without significant degradation of the mechanical properties across the entire diameter of the substrate.

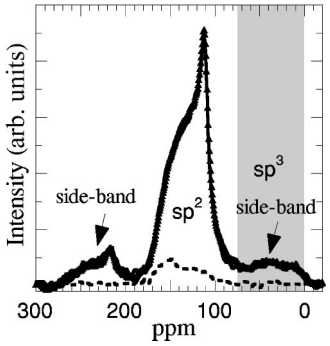


FIG. 2. $^{13}C$ Hahn echo MAS spectra of $a$-$CN_x$: $\tau_d$=10 s; $\tau_e$ =125 $\mu$s; $\nu_r$=8 kHz, and NS=20 000. Spectra are shown with proton decoupling (triangles) and without (solid line). The gray shading indicates the region were $sp^3$ carbon signals are expected. The low-intensity Hahn Echo CP-MAS spectrum (dashed line) was acquired with a 1-ms contact time: $\tau_d$=1 s; $\tau_e$=111.1 $\mu$s; $\nu_r$ =9 kHz; and NS=10 000. The CP-MAS spectrum has been multiplied by a factor of $\sqrt{2}$ to ensure the same signal-to-noise ratio in both spectrum.

A comparison of $^{13}C$ Hahn echo spectra obtained by direct detection and cross-polarization measurements (low-intensity dashed curve) is given in Fig. 2. The CP-MAS spectra (1 ms contact time) has been scaled by a factor of $\sqrt{2}$ to equalize the signal-to-noise ratio in both spectra. The lower relative intensity of the cross-polarization spectrum suggests that our $a$-$CN_x$ material is not significantly hydrogenated. This is further supported by the fact that the resolution and shape of the Hahn echo direct detection spectra is not altered by proton decoupling, as also shown in Fig. 2 (symbol and solid line). Since magnetization transfer is mediated by dipolar interactions, cross polarization is more efficient (intensity is higher) for carbons closer to protons. For a 1-ms contact time, the observed intensity is slightly higher at $\sim$150 ppm (dashed spectrum in Fig. 2). In addition, the sharper peak at $\sim$150 ppm is suppressed for the spectrum acquired at a 5 ms contact time (not shown). The higher cross-polarization efficiency of the feature at 150 ppm observed at shorter contact times indicates that those carbons that are protonated are also more likely to be directly bonded to nitrogen.

The low-intensity lobes that are positioned symmetrically around the central peak of the spectra in Fig. 2 are the spinning sidebands. Since the sidebands partially obscure the region of the spectrum where $sp^3$ bonded carbon resonates[22] (0–75 ppm), Hahn echo experiments were carried out at higher spinning speeds. Comparison of the spectra obtained at 8 and 10 kHz spinning speeds (Figs. 2 and 3, respectively)

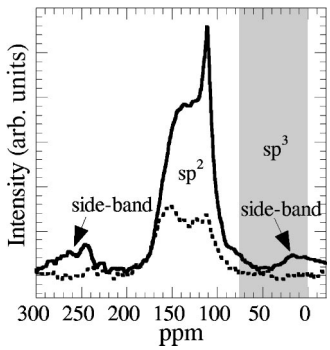


FIG. 3. Comparison of TOSS ($\tau_d = 3$ s, $\nu_r = 6$ kHz, NS $= 15\,000$, and dashed line) and Hahn echo (HE) MAS ($\nu_r = 10$ kHz, $\tau_d = 10$ s, $\tau_e = 200$ $\mu$s, and NS$= 10\,000$, and solid line). This figure shows that the small feature in the shaded $sp^3$ area of Fig. 2 is a spinning sideband. The spectra were scaled so that the noise level is approximately the same in each.

shows that the low-intensity feature between 0 and 75 ppm moves with respect to the central portion of the spectrum, as expected for a spinning sideband. Currently spinning speeds above 10 kHz are not available, so a TOSS sequence was implemented to completely suppress the sidebands. The TOSS spectrum (dashed line in Fig. 3) confirms the absence of $sp^3$ bonded carbon in hard and elastic $a$-$CN_x$. In addition, the ratio of the rms noise level with the intensity of the sharp peak at 112 ppm in the direct detection spectrum suggests an upper bound estimate of 0.1% for $sp^3$ carbon in this material.

The results of the dipolar dephasing REAPDOR experiment for $a$-$CN_x$ are shown in Fig. 4. The full spectrum (filled squares) is compared to the attenuated spectrum (open circles). The attenuated spectrum is obtained by applying an adiabatic-passage pulse to the $^{14}$N channel, which results in dipolar dephasing.[18] Since the strength of the dipolar interaction is inversely proportional to the cube of the internuclear bond distance, the carbons bonded closest to the nitrogen experience the strongest dipolar coupling. Thus, the highest dephasing efficiency (signal attenuation) is observed for the carbons bonded directly to nitrogen. The difference

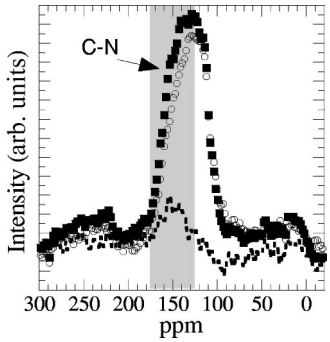


FIG. 4. Dipolar dephasing REAPDOR spectra were acquired with $\tau_d = 3$ s, $\nu_r = 8$ kHz, and NS$= 26\,000$. The full spectrum (filled squares), attenuated spectrum (open circles), and difference spectrum (dashed line) are shown. The gray-shaded region indicates the portion of the spectra attributed to carbon directly bonded to nitrogen.

spectrum between the full and attenuated spectra is shown in Fig. 4 (dashed line) corresponds to only those $^{13}$C coupled to $^{14}$N. The maximum observed dephasing at $\sim$150 ppm corresponds to carbon directly bonded to nitrogen. The minimum dephasing at 90–110 ppm corresponds to $sp^2$ carbon directly bonded to carbon. This information allows partial assignment of the direct detected Hahn echo spectrum (Fig. 2); the sharp peak at 110 ppm is now attributed to $sp^2$ carbon bonded to carbon, and the broad shoulder at 125–175 ppm is attributed to $sp^2$ carbon bonded to nitrogen. Interestingly, the CP-MAS indicates that the carbons bonded to nitrogen are also in closer proximity to protons, which suggests some of the nitrogen may be protonated; we are currently exploring this subject in more detail.

It is important to note that some of the changes in the shape and intensity observed among TOSS, REAPDOR, and Hahn echo direct detection spectra are due to the fact that for TOSS and REAPDOR data acquisition occurred after four and six rotor cycles, respectively. Since TOSS and REAPDOR are much longer pulse sequences, some distortions are anticipated due to $T_2$ differences for each bonding configuration.

Young-Gui *et al.* have calculated the chemical shifts of a variety of carbon nitride phases.[23] The calculated $^{13}$C chemical shift of graphitic $C_3N_4$ (144 ppm) is the only value that falls within the experimental spectral range. Interestingly, the graphitic phase of $C_3N_4$ consists of two nonequivalent nitrogen bonding sites around the perimeter of a vacancy defect structure: a site where N is coordinated to two carbons and a site where N is coordinated to three carbons. The computational work by Snis and Matar[24] on the model carbon nitride compound, $C_{11}N_4$, demonstrates an x-ray photoelectron spectroscopy (XPS) chemical shift of $\sim$2 eV between the two types of sites described above. This prediction is consistent with our experimental XPS spectra[4] of hard and elastic $a$-$CN_x$, and this suggests that the vacancy defect structures found in $C_3N_4$ and $C_{11}N_4$ may occur in $a$-$CN_x$ thin films.

## IV. CONCLUSIONS

In conclusion, in this paper we report $^{13}$C NMR characterization of hard and elastic amorphous carbon nitride, $a$-$CN_x$. Our results show that the material has an $sp^2$ carbon bonded structure and does not include any $sp^3$ hybridized carbon. Using double resonance techniques (REAPDOR), we were able to distinguish the $sp^2$ carbons bonded to other carbons from those bonded to nitrogen. The nanoindentation results demonstrate that this $a$-$CN_x$ material exhibits a high elastic recovery having a low modulus but high strength. The inferred $sp^2$ bonded carbon structure is consistent with the low-modulus structure similar to that of graphite, the stereotypical $sp^2$ hybridized carbon structure. However, the high elastic recovery is not observed in graphite. Our results elucidate the carbon hybridization in $a$-$CN_x$ thin films and highlight the important remaining questions about the structures responsible for the high elastic recovery in this material.

**ACKNOWLEDGMENTS**

The authors are thankful for the insightful comments and advice given by Professor R. L. Vold. This work was supported by the Jeffress Memorial trust (J-504), the NSF under Grant No. CHE-0079316 (G.L.H), the Research Corporation, and the American Chemical Society Petroleum Research Fund.

[1] H. Sjostrom, L. Hultman, J. E. Sundgren, S. V. Hainsworth, T. F. Page, and G. Theunissen, J. Vac. Sci. Technol. A **14**, 56 (1996).
[2] N. Hellgren, M. P. Johansson, E. Broitman, L. Hultman, and J. E. Sundgren, Phys. Rev. B **59**, 5162 (1999).
[3] B. C. Holloway, O. Kraft, D. K. Shuh, W. D. Nix, M. A. Kelly, P. Pianetta, and S. Hagstrom, J. Vac. Sci. Technol. A **18**, 2964 (2000).
[4] B. C. Holloway, O. Kraft, D. K. Shuh, W. D. Nix, M. A. Kelly, P. Pianetta, and S. Hagstrom, Appl. Phys. Lett. **74**, 3290 (1999).
[5] A. Johansson and S. Stafstrom, J. Chem. Phys. **111**, 3203 (1999).
[6] L. Hultman, S. Stafstrom, Z. Czigany, J. Neidhardt, N. Hellgren, I. F. Brunell, K. Suenaga, and C. Colliex, Phys. Rev. Lett. **87**, 225503 (2001).
[7] L. Wan and R. F. Egerton, Thin Solid Films **279**, 34 (1996).
[8] C. Spaeth, M. Kuhn, F. Richter, U. Falke, M. Hietschold, R. Kilper, and U. Kreissig, Diamond Relat. Mater. **7**, 1727 (1998).
[9] W. T. Zheng, W. X. Yu, H. B. Li, Y. M. Wang, P. J. Cao, Z. S. Jin, E. Broitman, and J. E. Sundgren, Diamond Relat. Mater. **9**, 1790 (2000).
[10] H. Jiangtao, Y. Peidong, and C. M. Lieber, Phys. Rev. B **57**, R3185 (1998).
[11] L. Dong, C. Yip-Wah, Y. Shengtian, W. Ming-Show, F. Adibi, and W. D. Sproul, J. Vac. Sci. Technol. A **12**, 1470 (1994).
[12] J. LaManna, J. Braddock-Wilking, S. H. Lin, and B. J. Feldman, Solid State Commun. **109**, 573 (1999).
[13] S. H. Lin, J. Braddock-Wilking, and B. J. Feldman, Solid State Commun. **114**, 193 (2000).
[14] J. C. Sanchez-Lopez, C. Donnet, F. Lefebvre, C. Fernandez-Ramos, and A. Fernandez, J. Appl. Phys. **90**, 675 (2001).
[15] E. Broitman, N. Hellgren, O. Wanstrand, M. P. Johansson, T. Berlind, H. Sjostrom, J. E. Sundgren, M. Larsson, and L. Hultman, Wear **248**, 55 (2001).
[16] N. Hellgren, M. P. Johansson, B. Hjorvarsson, E. Broitman, M. Ostblom, B. Liedberg, L. Hultman, and J. E. Sundgren, J. Vac. Sci. Technol. A **18**, 2349 (2000).
[17] S. J. Lang, J. Magn. Reson., Ser. A **104**, 345 (1993).
[18] B. Yong, K. Hsien-Ming, C. P. Grey, L. Chopin, and T. Gullion, J. Magn. Reson. **133**, 104 (1998).
[19] W. C. Oliver and G. M. Pharr, J. Mater. Res. **7**, 1564 (1992).
[20] N. Hellgren, K. Macak, E. Broitman, M. P. Johansson, L. Hultman, and J. E. Sundgren, J. Appl. Phys. **88**, 524 (2000).
[21] W. T. Zheng, H. Sjostrom, I. Ivanov, K. Z. Xing, E. Broitman, W. R. Salaneck, J. E. Greene, and J. E. Sundgren, J. Vac. Sci. Technol. A **14**, 2696 (1996).
[22] D. E. Leydon and R. H. Cox, *Analytical Applications of NMR* (Wiley, New York, 1977), Vol. 48, p. 196.
[23] Y. Young-Gui, B. G. Pfrommer, F. Mauri, and S. G. Louie, Phys. Rev. Lett. **80**, 3388 (1998).
[24] A. Snis and S. F. Matar, Phys. Rev. B **60**, 10 855 (1999).